

Self-Assembly of Highly Oriented Lamellar Nanoparticle-Phospholipid Nanocomposites on Solid Surfaces

Bing Yuan, Li-Li Xing, Yu-Dong Zhang, Ying Lu, Zhen-Hong Mai, and Ming Li*

Beijing National Laboratory for Condensed Matter Physics, Institute of Physics, Chinese Academy of Sciences, Beijing 100080, China

Received June 11, 2007; E-mail: mingli@aphy.iphy.ac.cn

When nanoparticles (NPs) are embedded in organic matrices, the materials can show not only combined properties of the original components but also improved performances not seen in the original components.¹ To this end, it is important to control the size, shape, and dispersion of the NPs on a chemically diverse range of supports. However, controlling materials at the nanometer scale is of great challenge, particularly when long-range ordering is pursued. In most of the studies, the NPs are synthesized *in situ*, and it is difficult to control their size distribution and dispersion on the support.^{1,2} As monodisperse NPs can nowadays be routinely synthesized, more researchers are trying to use self-assembly,³ field-directed deposition,⁴ template-directed self-assembly,⁵ and layer-by-layer assembly⁶ to fabricate NP-containing composites. In most of the methods, complicated processing procedures and/or charge matching are required, but a well-dispersed structure with long-range ordering has seldom been obtained.

In this work, we exploit the self-assembly property of amphiphilic molecules to disperse water-soluble NPs. The self-assembly allows the production of ordered lamellar structure without the requirement of high-precision patterning and/or opposite-charge matching. In our method, a drop of a mixed solution of NPs and phospholipids was cast onto the surface of a silicon or glass wafer. Multilayered nanocomposite was formed after the rapid evaporation of water in the evacuated chamber (Figure 1a). The phospholipid used is dioleoyl-*sn*-glycero-phosphocholine (DOPC), and the original NP solution is CdTe suspension in water (~ 3 nm in diameter, stabilized with 3-mercaptopropionic acid, and negatively charged because of the carboxy groups on the surface). The process begins with a DOPC solution of an initial concentration ($c_0 = 2.0$ mg/mL) higher than the critical micelle concentration, and sonication results in formation of micelles and liposomes. The added NPs adsorb onto the membranes to form stable nanoparticle-liposome hybrids in the solution.⁷ When cast onto a hydrophilic surface, the solution outspreads over the solid surface. Evaporation-induced enrichment of the phospholipids leads to conglutination and fusion of the liposomes (with the adsorbed NPs), and promotes cooperative assembly of the molecules into a liquid-crystalline mesophase with the NPs being confined in the hydrophilic interfaces. The rapid solvent evaporation is believed to be crucial for the assembly process (Supporting Information), making them different from the assembly of DNA/lipid complexes in solutions.⁸ The evaporation is faster at the edge than in the interior of the spreading fluid. An outward flow of the solvent develops because the solvent removed via evaporation must be replenished by a flow from the interior.^{3c} The flow endows a shear on the lamellar mesophase, aligning all the interfaces parallel to the solid surface.

The cross-section TEM images in Figure 1 show clearly well-defined lamellar distribution of the NPs. The phospholipids are invisible in the TEM images, but the observed fluctuation of the layers and variation of the interlayer distances are intrinsic to them.

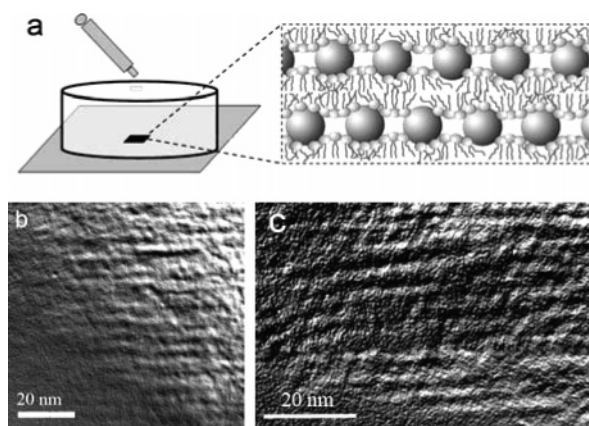


Figure 1. (a) Cartoons showing the fabrication process and the structural model of the nanocomposite. (b, c) Cross-section TEM images of two typical samples.

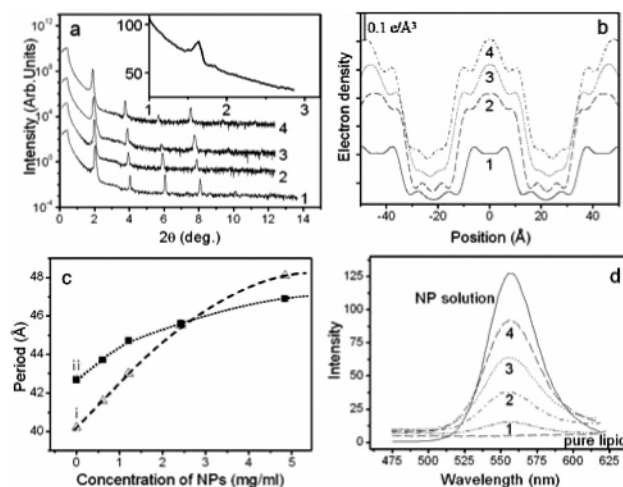


Figure 2. (a) XRR patterns of the samples with different NP concentrations: (1) 0.6, (2) 1.2, (3) 2.4, (4) 4.8 mg/mL. The concentration of phospholipids is 2.0 mg/mL for all the samples. Inset shows the GIXRD pattern of sample 3, indicating that the NPs are two-dimensionally ordered. (b) EDP from the reflectivity data. (c) Period vs NP concentration for different phospholipid templates: (i) DOPC/DOTAP = 8:2, and (ii) pure DOPC. (d) PL spectra of the samples. The spectra of a pure lipid film and the NP solution are given for reference. The numbers in panels b and d have the same meaning as those in panel a. The curves in panels a and b are offset for clarity.

The X-ray reflectivity (XRR) analysis confirms that the structure is homogeneous and highly ordered. The grazing incident X-ray diffraction (GIXRD) measurements reveal a peak at 1.63° (inset in Figure 2a), indicating that the NPs are two dimensionally ordered at the interfaces between the lipid bilayers. The period of the film increases gradually from 42.7 Å (for pure lipid film) to 46.9 Å

(curve 4 in Figure 2a) as the NPs concentration in the mixed solution increases from 0 to 4.8 mg/mL. Assuming a linear dependence of the increase in period on the amount of incorporated NPs, we can estimate the interparticle separation to be about 11, 8, 6, and 5 nm, respectively, for the samples in Figure 2a. The values are in agreement with the GIXRD measurements assuming that the NPs are hexagonally close packaged. It is of practical importance to control the interparticle separation because it provides a means to tune both the quantum and classical coupling interactions between the NPs, and in turn, to tune the electronic and magnetic properties of the hybrid nanostructures.⁹ The interparticle separation can be readily controlled by adjusting the concentrations of the NPs and the lipids in the mixed solutions. It will be shown later that addition of charged lipids into the membranes can greatly improve the incorporation ability of the NPs, which can also be used to adjust the interparticle separation.

XRR is sensitive to the electron density profile (EDP) of the multilayers which can be obtained by fitting the reflectivity data.¹⁰ The EDPs in Figure 2b reveal that the NPs are located between the bilayers. The effective distance between the headgroups is significantly increased from 6.2 Å (for pure lipid film) to 20.1 Å (for curve 4 in Figure 2b) upon incorporation of the NPs. The tails of the lipids are compressed as a consequence of crowding by the NPs. Nevertheless, the effective interface between the NP-layer and the lipid bilayer is clearly seen in the EDPs, suggesting the lipid bilayers are not severely disturbed. This is not surprising because a stable bilayer can be formed even on the surface of a colloidal crystal¹¹ owing to the elasticity of the bilayers. The densities corresponding to the headgroup regions in Figure 2b increase gradually from curve 1 to 4 owing to the contribution from the NPs.

The adsorption of the NPs to the liposomes is believed to be essential for forming the hybrid multilayers. The driving force for the adsorption could be either the entropy increase due to displacement of water molecules by the adsorbed NPs on the hydrated (neutral) membrane surfaces or charge-dipole attraction between the charged NPs and the phosphor-nitrogen dipole of the phospholipid headgroups.⁷ When neutral DOPC is mixed with 1,2-dioleoyl-3-trimethylammonium-propane (DOTAP, positively charged), more NPs can be incorporated into the multilayers. In Figure 2c, curves i and ii are the period vs NP concentration plots for the nanocomposites with and without DOTAP, respectively. The period of the DOPC-DOTAP multilayer is smaller than that of the DOPC multilayer because the headgroup of DOTAP is shorter than that of DOPC. But when the NPs are added, the period of the DOPC-DOTAP/NP films increases faster than that of the DOPC/NP films, indicating that, in the present of DOTAP, the admitting ability of the nanocomposite for the NPs is enhanced. Such an enhancement may come from the electrostatic interaction between them because the NPs are negatively charged.

The photoluminescence (PL) spectra of the nanocomposites with different amount of NPs are shown in Figure 2d. They are characteristic of the NPs. No red-shift of the PL relative to that of the original solution is observed, indicating that aggregation of the NPs does not occur inside the nanocomposites.¹² The PL of the NPs in the as-cast nanocomposites is initially weak and broad. But upon photoirradiation for ~15 min in vacuum, the PL recovered to a level similar to that in the original solution (Supporting Information). The phenomenon may arise from photoinduced surface reconstruction of the NPs, or surface-ligand passivation induced by photon-phonon coupling.¹³ This could potentially be exploited for the development of gas-sensing technologies^{13a}

because the PL properties can respond reversibly and reproducibly to environmental changes upon photoirradiation.

In summary, we report on a new and versatile method to disperse NPs into ordered lamellar structures. The period of the nanocomposites and the 2D interparticle separation can be tuned by adjusting the concentration of the NPs relative to that of the surfactants and/or by incorporating charged surfactants. As NPs can carry many different functions and can be chemically activated or loaded, the combination of organic reagents with NPs in layered composites would open a wide playground where structures, functions, and, ultimately, properties can be controlled.^{13b,14} The biocompatibility of the phospholipid membranes promises also potential applications in biology.¹⁵ The constituent elements of the nanocomposites are not restricted to phospholipids and semiconductor NPs.¹⁶ The combination of various surfactants with different kinds of target particles, ranging from biomolecules and viruses to quantum dots and nanotubes, will certainly broaden the application of the nanocomposites.

Acknowledgment. This work was financially supported by the National Natural Science Foundation of China (Grant Nos. 10325419, 10674158, and 10574159) and by the Knowledge Innovation Program of the Chinese Academy of Sciences (Grant No. kjcx3.syw.n8). The NPs are a gift of Dr. L. Feng of the Tsinghua University, China. The X-ray measurement was performed at the Beijing Synchrotron Radiation Facility (BSRF).

Supporting Information Available: Materials and sample preparation, PL spectrum, XRR of samples with combination of different surfactants, supplementary discussion. This material is available free of charge via the Internet at <http://pubs.acs.org>.

References

- (1) Zhou, Y.; Kogiso, M.; He, C.; Shimizu, Y.; Koshizaki, N.; Shimizu, T. *Adv. Mat.* **2007**, *19*, 1055.
- (2) (a) Shi, F.; Zhang, Q. H.; Ma, Y. B.; He, Y. D.; Deng, Y. Q. *J. Am. Chem. Soc.* **2005**, *127*, 4182. (b) Zheng, N. F.; Stucky, G. D. *J. Am. Chem. Soc.* **2006**, *128*, 14278.
- (3) (a) Banfield, J. F.; Welch, S. A.; Zhang, H. Z.; Ebert, T. T.; Penn, R. L. *Science* **2000**, *289*, 751. (b) Tang, Z. Y.; Kotov, N. A.; Giersig, M. *Science* **2002**, *297*, 237. (c) Govor, L. V.; Reiter, G.; Parisi, J.; Bauer, G. H. *Phys. Rev. E* **2004**, *69*, No. 061609.
- (4) (a) Wu, L. Q.; Lee, K.; Wang, X.; English, D. S.; Losert, W.; Payne, G. F. *Langmuir* **2005**, *21*, 3641. (b) Aldaye, F. A.; Sleiman, H. F. *J. Am. Chem. Soc.* **2007**, *129*, 4130.
- (5) (a) Chiu, J. J.; Kim, B. J.; Kramer, E. J.; Pine, D. J. *J. Am. Chem. Soc.* **2005**, *127*, 5036. (b) Chiu, J. J.; Kim, B. J.; Yi, G. R.; Bang, J.; Kramer, E. J.; Pine, D. J. *Macromolecules* **2007**, *40*, 3361.
- (6) (a) Schmitt, J.; Decher, G.; Dressick, W. J.; Brandow, S. L.; Geer, R. E.; Shashidhar, R.; Calvert, J. M. *Adv. Mat.* **1997**, *9*, 61. (b) Fendler, J. H. *Chem. Mater.* **2001**, *13*, 3196. (c) Krishnan, R. S.; Mackay, M. E.; Duxbury, P. M.; Pastor, A.; Hawker, C. J.; Van Horn, B.; Wong, M. S.; Asokan, S. *Nano. Lett.* **2007**, *7*, 484.
- (7) Zhang, L. F.; Granick, S. *Nano. Lett.* **2006**, *6*, 694.
- (8) (a) Radler, J. O.; Koltover, I.; Salditt, T.; Safinya, C. R. *Science* **1997**, *275*, 810. (b) Safinya, C. R. *Curr. Opin. Struct. Biol.* **2001**, *11*, 440.
- (9) (a) Collier, C. P.; Saykally, R. J.; Shiang, J. J.; Henrichs, S. E.; Heath, J. R. *Science* **1997**, *277*, 1978. (b) Shenhar, R.; Norsten, T. B.; Rotello, V. M. *Adv. Mater.* **2005**, *17*, 657. (c) Aldaye, F. A.; Sleiman, H. F. *J. Am. Chem. Soc.* **2007**, *129*, 4130.
- (10) Xing, L. L.; Li, D. P.; Hu, S. X.; Jing, H. Y.; Fu, H. L.; Mai, Z. H.; Li, M. *J. Am. Chem. Soc.* **2006**, *128*, 1749.
- (11) Brozell, A. M.; Muha, M. A.; Sani, B.; Parikh, A. N. *J. Am. Chem. Soc.* **2006**, *128*, 62–63.
- (12) (a) Zaitseva, N.; Dai, Z. R.; Leon, F. R.; Krol, D. J. *J. Am. Chem. Soc.* **2005**, *127*, 10221. (b) Kagan, C. R.; Murray, C. B.; Nirmal, M.; Bawendi, M. G. *Phys. Rev. Lett.* **1996**, *76*, 1517.
- (13) (a) Nazzari, A. Y.; Qu, L.; Peng, X.; Xiao, M. *Nano. Lett.* **2003**, *3*, 819. (b) Balazs, A. C. *Nat. Mater.* **2007**, *6*, 94.
- (14) Warren, S. C.; Disalvo, F. J.; Wiesner, U. *Nat. Mater.* **2007**, *6*, 156.
- (15) Terheiden, A.; Mayer, C.; Moh, K.; Stahlmecke, B.; Stappert, S.; Acet, M. *Appl. Phys. Lett.* **2004**, *84*, 3891.
- (16) Combination of phospholipids with surfactants such as cetyl trimethyl ammonium bromide (CTAB, positively charged) or sodium dodecyl sulfate (SDS, negatively charged) as well as pure CTAB were also used as templates in our experiments (Supporting Information).

JA074235N